2013

Magnetic field induced discontinuous spin reorientation in ErFeO3 single crystal

Hui Shen
Shanghai Institute Of Technology, huishen@uow.edu.au

Zhenxiang Cheng
University of Wollongong, cheng@uow.edu.au

Fang Hong
University of Wollongong, fh640@uowmail.edu.au

Jiayue Xu
Chinese Academy Of Sciences,Shanghai Institute Of Technology

Shujuan Yuan
Shanghai University

See next page for additional authors

Publication Details

Shen, H., Cheng, Z., Hong, F., Xu, J. Y., Yuan, S., Cao, S. X. & Wang, X. (2013). Magnetic field induced discontinuous spin reorientation in ErFeO3 single crystal. Applied Physics Letters, 103 192404-1-192404-5.

Magnetic field induced discontinuous spin reorientation in ErFeO3 single crystal

Abstract
The spin reorientation of ErFeO3 that spontaneously occurs at low temperature has been previously determined to be a process involving the continuous rotation of Fe3þ spins. In this work, the dynamic process of spin reorientation in ErFeO3 single crystal has been investigated by AC susceptibility measurements at various frequencies and static magnetic fields. Interestingly, two completely discontinuous steps are induced by a relatively large static magnetic field due to the variation in the magnetic anisotropy during this process. It provides deeper insights into the intriguing magnetic exchange interactions which dominate the sophisticated magnetic phase transitions in the orthoferrite systems.

Keywords
field, induced, discontinuous, magnetic, spin, crystal, reorientation, erfeo3, single

Disciplines
Engineering | Physical Sciences and Mathematics

Publication Details
Shen, H., Cheng, Z., Hong, F., Xu, J. Y., Yuan, S., Cao, S. X. & Wang, X. (2013). Magnetic field induced discontinuous spin reorientation in ErFeO3 single crystal. Applied Physics Letters, 103 192404-1-192404-5.

Authors
Hui Shen, Zhenxiang Cheng, Fang Hong, Jiayue Xu, Shujuan Yuan, Shixun Cao, and Xiaolin Wang

AIP | Applied Physics Letters

Magnetic field induced discontinuous spin reorientation in ErFeO3 single crystal

Hui Shen, Zhenxiang Cheng, Fang Hong, Jiayue Xu, Shujuan Yuan, Shixun Cao, and Xiaolin Wang

Citation: Applied Physics Letters **103**, 192404 (2013); doi: 10.1063/1.4829468
View online: http://dx.doi.org/10.1063/1.4829468
View Table of Contents: http://scitation.aip.org/content/aip/journal/apl/103/19?ver=pdfcov
Published by the AIP Publishing

Magnetic field induced discontinuous spin reorientation in $ErFeO_3$ single crystal

Hui Shen,[1,2] Zhenxiang Cheng,[2,a)] Fang Hong,[2] Jiayue Xu,[1] Shujuan Yuan,[3] Shixun Cao,[3] and Xiaolin Wang[2]

[1]*School of Materials Science and Engineering, Shanghai Institute of Technology, Shanghai 201418, People's Republic of China*

[2]*Institute for Superconducting and Electronic Materials, University of Wollongong, NSW 2500, Australia*

[3]*Department of Physics, Shanghai University, Shanghai 200444, People's Republic of China*

(Received 28 September 2013; accepted 24 October 2013; published online 7 November 2013)

The spin reorientation of $ErFeO_3$ that spontaneously occurs at low temperature has been previously determined to be a process involving the continuous rotation of Fe^{3+} spins. In this work, the dynamic process of spin reorientation in $ErFeO_3$ single crystal has been investigated by AC susceptibility measurements at various frequencies and static magnetic fields. Interestingly, two completely discontinuous steps are induced by a relatively large static magnetic field due to the variation in the magnetic anisotropy during this process. It provides deeper insights into the intriguing magnetic exchange interactions which dominate the sophisticated magnetic phase transitions in the orthoferrite systems. © *2013 AIP Publishing LLC*. [http://dx.doi.org/10.1063/1.4829468]

In recent years, orthoferrites ($RFeO_3$, R = rare earths) with the *Pbnm* structure have gained renewed interest, thanks to their unique physical properties and some potential applications, such as in multiferroics, ultra-fast photomagnetic excitation, and ultra-fast spin switching.[1–5] Some of them surprisingly display magnetic ordering induced ferroelectric polarization. In $GdFeO_3$ single crystal, ferroelectric polarization and magnetization have been successfully controlled by magnetic and electric fields, respectively, which is attributed to the unique feature of composite domain wall clamping of the respective domain walls for the electric and magnetic orders.[1] A magnetic field along the *c*-axis of $DyFeO_3$ single crystal can induce a gigantic magnetoelectric coupling, which is driven by the exchange striction mechanism.[6,7] Room temperature ferroelectricity is observed in $SmFeO_3$, and the canted antiferromagnetic ordering is responsible for this extraordinary polarization.[8] This system is also the subject of considerable research aimed at better understanding of the complex and competing magnetic interactions, which can be modified by many parameters, such as the doping level, temperature, field, and pressure. For example, substitution of Mn in non-multiferroic $YFeO_3$ ($YFe_{0.6}Mn_{0.4}O_3$) effectively induces large magnetocapacitance (18% at 50 kOe) at 320 K and ferroelectricity with a relatively high ferroelectric transition temperature (~115 K).[9] The electronic structure of $ErFeO_3$ has been studied by spectroscopic ellipsometry, showing the charge transfer transitions in octahedral FeO_6 centers.[10]

Spin reorientation is another attractive characteristic of $RFeO_3$, in which the direction of the easy axis of magnetization changes from one crystal axis to another.[11,12] The following three types of *G*-type antiferromagnetic (AFM) configurations can be observed for orthoferrites: $\Gamma_1(A_x, G_y, C_z)$, $\Gamma_2(F_x, C_y, G_z)$, and $\Gamma_4(G_x, A_y, F_z)$, following the Bertaut notation.[13] Γ_4 is the basal magnetic structure of Fe^{3+} just below the Néel temperature, T_N, which is a canted AFM structure with a total ferromagnetic (FM) vector ***F*** directed along the *c* (*c*//*z*) crystal axis, and an AFM vector ***G*** directed along the *a* (*a*//*x*) crystal axis.[14] For non-magnetic R^{3+} othoferrites ($YFeO_3$, $LaFeO_3$, and $LuFeO_3$) and some magnetic R^{3+} othoferrites ($GdFeO_3$, $EuFeO_3$, and $PrFeO_3$), Γ_4 is retained down to the lowest temperature. $DyFeO_3$ is the only orthoferrite to show a Morin transition, where the Fe^{3+} system spins are reoriented from Γ_4 to $\Gamma_1$around 35 K, at which the AFM spins rotate from the *a*-axis to the *b*-axis.[15] For all other orthoferrites, such as $ErFeO_3$, it is commonly believed that the FM vector ***F*** continuously rotates from the *c*-axis (Γ_4) towards the *a*-axis (Γ_2) while staying in the *ac*-plane through the intermediate phase ($\Gamma_{24}(G_{xz}, F_{xz})$),[16,17] upon cooling below its Néel temperature, as seen in Fig. 1.

At present, interest in the spin reorientation of orthoferrites is being greatly revived because this transition is closely related to the magnetically driven ferroelectricity. Moreover, laser induced ultra-fast control of this transition has been reported in several orthoferrites, including $DyFeO_3$, $TmFeO_3$, and also $ErFeO_3$.[3,18,19] In order to uncover the mechanism of this process, the spin dynamics have been investigated by several kinds of technological methods, including terahertz time

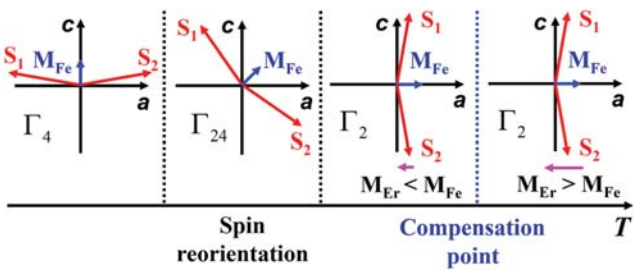

FIG. 1. Simplified magnetic configuration of $ErFeO_3$ upon cooling below T_N; the black arrow at the bottom indicates the decreasing temperature; S_1 and S_2 are the two pairs of spins for Fe^{3+} in the *G*-type AFM; M_{Fe} is the net FM moment of Fe^{3+} for $ErFeO_3$, and M_{Er} is the moment of Er^{3+}.

a)Author to whom correspondence should be addressed. Electronic mail: cheng@uow.edu.au

domain spectroscopy, ultrafast laser pulses, neutron diffraction, etc.[19–21] In AC measurements, an oscillating component is added to the static magnetic field, causing a time-dependent moment in the sample, which is a very sensitive probe for detecting a magnetic phase transition initiated by a change in the magnetocrystalline anisotropy energy.[22] The spin reorientation process in $ErFeO_3$ that spontaneously occurs at low temperature has been previously determined to be a continuous and coherent rotation of Fe^{3+}.[23] In the present work, an interesting phenomenon, the discontinuous rotation of Fe^{3+} spins in $ErFeO_3$, has been observed in AC magnetic susceptibility measurements. The possible mechanism for this dynamic process is also proposed.

The material studied in this work is $ErFeO_3$ single crystal. The starting materials for the preparation of feed and seed rods for the floating zone crystal growth were powders of Er_2O_3 (99.9%) and Fe_2O_3 (99.99%). The raw materials were manually mixed in stoichiometric amounts and calcined at 1200 °C for 24 h in air. After cooling down to room temperature, these samples were thoroughly reground and pressed into a rod with a diameter of 8 mm and a length of 10 cm. Then, the rod was sintered at 1400 °C for 24 h in air in order to obtain high quality polycrystalline rods. Single crystals were grown by the floating zone method using an image furnace (Crystal System Inc.). The magnetic measurements were carried out using a 9 T physical properties measurement system (PPMS; Quantum Design). In zero-field cooled (ZFC) measurements of magnetization, the sample was cooled down to 5 K without magnetic field, and the measurements were performed in the warming up process in applied magnetic field. For the field cooled (FC) conditions, the samples were first cooled down to 5 K in cooling fields, and then the measurements were performed in warming-up mode. The AC susceptibility was measured in frequencies ranging from 100 Hz to 5000 Hz while the sample was heated from 83 K to 105 K with ac excitation amplitude (H_{ac}) of 1 Oe and static magnetic field (H_{dc}) of 0 Oe to 1000 Oe.

Figs. 2(a) and 2(b) display the temperature dependence of the ZFC and FC magnetization for $ErFeO_3$ single crystal at different magnetic fields (H) of 200 Oe and 1000 Oe. Below its Néel ($T_N \approx 640$ K) temperature, the Fe^{3+} sublattice is in a canted G-type AFM ordering, resulting in a weak FM.[24] This can be proved by the hysteresis loop measured at 300 K, as shown in Fig. 2(c). A characteristic feature of R_mFeO_3 (R_m^{3+}, magnetic rare earth ion) is the presence of two magnetic sublattices of Fe^{3+} and R_m^{3+}, in which Fe^{3+}–Fe^{3+}, R_m^{3+}–Fe^{3+}, and R_m^{3+}–R_m^{3+} exchange interactions coexist. The competition between these interactions gives rise to interesting and complex magnetic properties. Among these interactions, the Fe^{3+}–O–Fe^{3+} superexchange interaction in $ErFeO_3$ is the dominant one, with Fe^{3+}–O–Fe^{3+} bond angle close to 144°,[25] which contributes to the AFM ordering with a weak FM component. The weak FM is attributed to the antisymmetric Dzyaloshinskii–Moriya (DM) exchange interaction ($D_i \bullet S_i \times S_j$) (where D_i is the exchange interaction intensity, and S_i and S_j are the two nearest spins) between neighbouring spins induced by the spin-orbit interaction, which reflects the local crystal anisotropy.[11]

In Figs. 2(a) and 2(b), sudden changes of magnetic moment were observed around 87 K and 97 K, which is in good agreement with the temperature interval of the spin reorientation of $ErFeO_3$.[16,26] With decreasing temperature below T_N, Er^{3+} is expected to be increasingly polarized, and its effective anisotropy increases, leading to the reorientation of the magnetization of Fe^{3+}. With further decreasing temperature, the magnetic moment decreases sharply and approaches zero around 50 K for $H = 200$ Oe and around 75 K for $H = 1000$ Oe. This indicates that the net moments of Fe^{3+} and Er^{3+} are antiparallel to each other due to the superexchange interaction, which is also shown in Fig. 1. The Er^{3+} ions only order below 4.4 K.[19] This interaction is relatively weak, and the Er^{3+} magnetization can be negligible

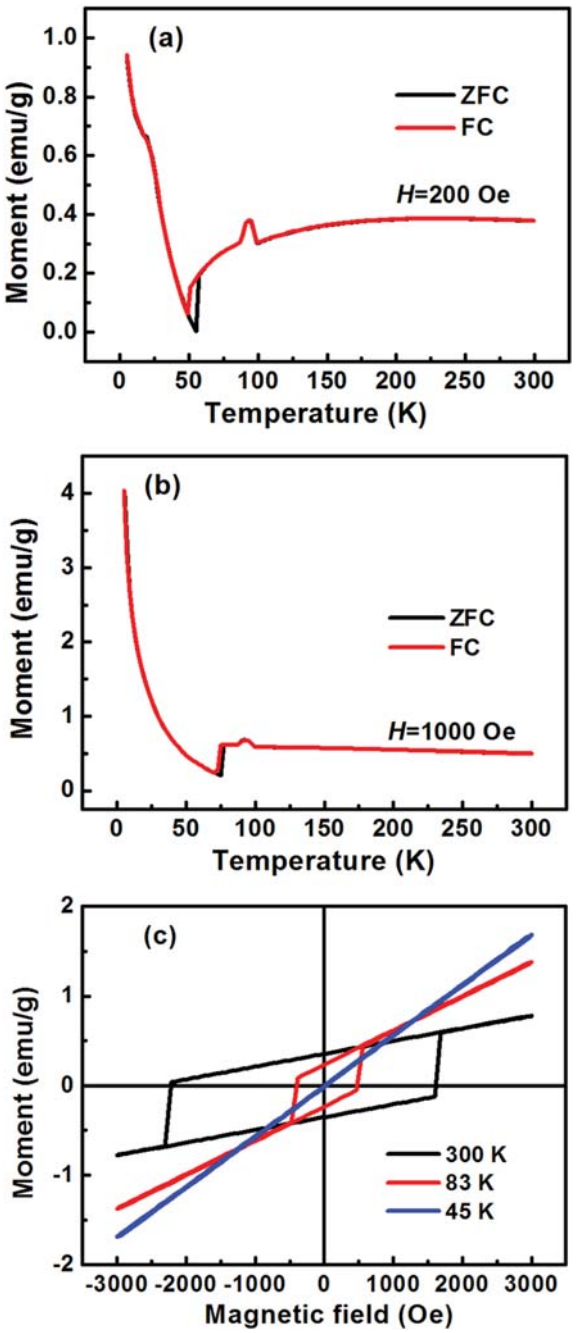

FIG. 2. Temperature dependence of the magnetization of $ErFeO_3$ single crystal measured in external field of (a) $H = 200$ Oe and (b) $H = 1000$ Oe. (c) Magnetic hysteresis loops measured at 300 K, 83 K, and 45 K with measuring field of ±3000 Oe.

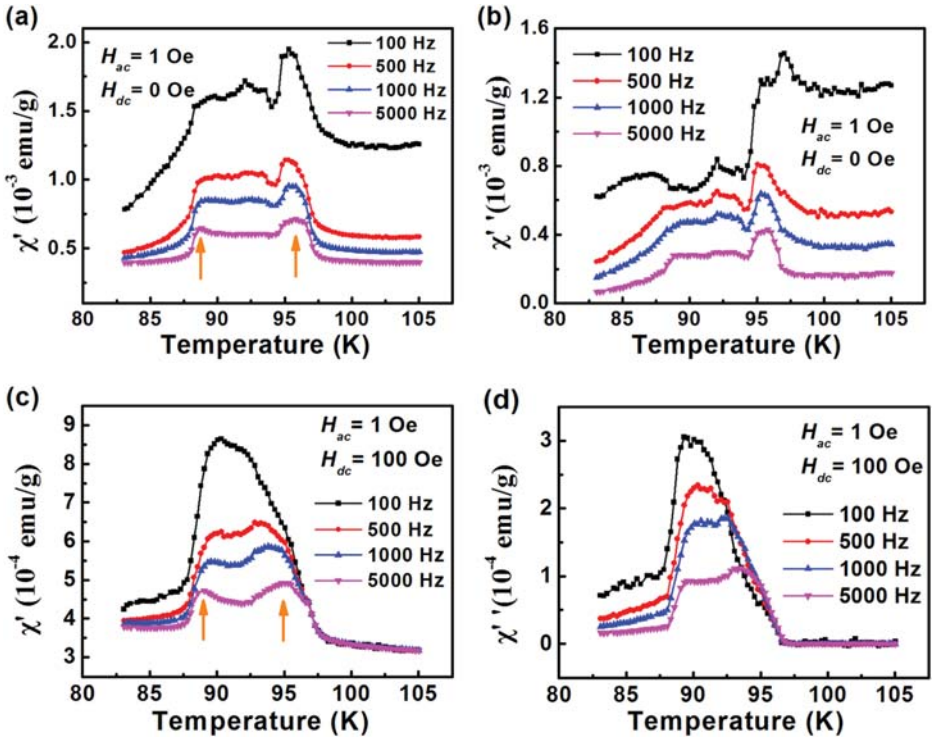

FIG. 3. Real part (a) and imaginary part (b) of the AC susceptibility of $ErFeO_3$ as a function of temperature at $H_{ac} = 1$ Oe and $H_{dc} = 0$ Oe at different frequencies; the real part (c) and imaginary part (d) of the AC susceptibility of $ErFeO_3$ as a function of temperature at $H_{ac} = 1$ Oe and $H_{dc} = 100$ Oe at different frequencies. The arrows indicate the two peaks.

above 100 K. As the temperature decreases, however, the magnetization of Er^{3+} increases, and the total moments of the Fe^{3+} and Er^{3+} sublattices are cancelled at a point called the compensation point.[27] Thereafter, the paramagnetic characteristics of the curve mainly originate from the larger magnetic moment of Er^{3+} ($9.59\mu_B/Er^{3+}$, $5.9\mu_B/Fe^{3+}$), which is gradually enhanced with decreasing temperature. As shown in Fig. 2(c), linear behaviour of the magnetic hysteresis loop was observed at 45 K, confirming the characteristics of the paramagnetic state below the compensation point. In Figs. 2(a) and 2(b), neither a divergence between the FC and ZFC curves nor a cusp in the ZFC curve are observed, which rules out spin-glass-like behaviour in $ErFeO_3$.

The dynamic process of spin reorientation in $ErFeO_3$ single crystal was systematically investigated by AC susceptibility measurements with varied H_{dc} and at various frequencies. Figs. 3(a) and 3(b) show the real part ($\chi'(T)$) and imaginary part ($\chi''(T)$) of the AC susceptibility of $ErFeO_3$ as a function of temperature at $H_{ac} = 1$ Oe and $H_{dc} = 0$ Oe, for various frequencies from 100 Hz to 5000 Hz. The real part χ' is the initial susceptibility, which is related to the variation in the sample magnetization, and χ'' is non-zero if the magnetic energy is absorbed by the sample.[28] With zero static magnetic field, a clear peak is observed around 96 K where the starting of the spin reorientation occurs. With decreasing temperature, both χ' (T) and χ'' (T) change slightly to form plateau-like peaks. Thereafter, they decrease steeply at the end of this transition, showing another peak at about 87 K. The position of the platform shows almost no dependence on the frequency of the oscillating field. It is noticeable, however, that there is a two-step process during the rotation of the FM vector $\boldsymbol{F}$ from the c-axis towards a-axis. The AC susceptibility of $TmFeO_3$ single crystal also changes irregularly with temperature, with a step-like shape.[29] This suggests a well-developed and rich magnetic structure in that particular temperature region.

The static magnetic field has especially strong effects on the dynamic susceptibility of $ErFeO_3$ in the spin reorientation temperature region (87 K–97 K). When H_{dc} increases to 100 Oe, the two-step process becomes more distinctive, as seen in Figs. 3(c) and 3(d). With increasing frequency, the peak at low temperature shifts to lower temperature while the peak at high temperature moves to higher temperature, resulting in greater separation of the two peaks. Similar

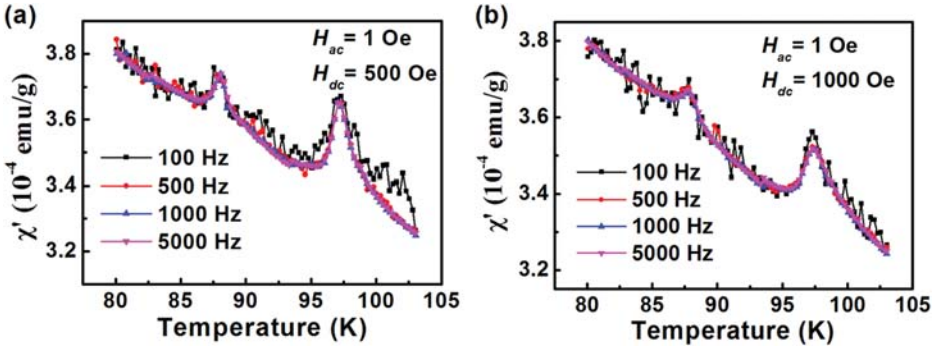

FIG. 4. Real part of the AC susceptibility of $ErFeO_3$ as a function of temperature at different frequencies: (a) $H_{ac} = 1$ Oe and $H_{dc} = 500$ Oe; (b) $H_{ac} = 1$ Oe and $H_{dc} = 1000$ Oe.

behaviour was also observed in $TbFeO_3$ at $2.8\,K \leq T \leq 10\,K$.[30] The slope change in the $\chi'(T)$ and the relatively large maximum of $\chi''(T)$ around 3.6 K are believed to be originated from the ordering of Tb^{3+}. Long-range ordering of Er^{3+}, however, does not occur in the temperature range for the spin reorientation of $ErFeO_3$. The spin reorientation of $ErFeO_3$ is mainly related to the rotation of the ferromagnetic vector $\boldsymbol{F}$ of Fe^{3+}. When H_{dc} continues to increase to 500 Oe and 1000 Oe, two completely distinctive peaks are formed at 87 K and 97 K, as shown in Figs. 4(a) and 4(b). This indicates that at higher static magnetic field, discontinuous rotations of the FM vector occur at the beginning and end of the spin reorientation.

The spin reorientation in $ErFeO_3$ reflects the exchange anisotropy evolution with temperature, which emerges from the strong competition between the two magnetic sublattices (Fe^{3+} and Er^{3+}). According to the *M-H* hysteresis loops shown in Fig. 2(c), the coercive field at 300 K (above the spin reorientation temperature) is much larger than that at 83 K (below the spin reorientation temperature), which indicates that the magnetic anisotropy of Γ_4 is larger than that of Γ_2. Both $\Gamma_4$and Γ_2 are stable magnetic states for $ErFeO_3$, with FM vector $\boldsymbol{F}$ along the *c* and *a* crystal axes, respectively. In the temperature region of 87 K–97 K, the intermediate state is metastable, and its anisotropy is expected to be determined by the competition between Γ_4 and Γ_2 during the rotation of the FM vector $\boldsymbol{F}$. With decreasing temperature below T_N, due to the large anisotropy and strong pinning force, it is difficult to rotate the FM vector of Fe^{3+} from the *c*-axis at the beginning of the transition. So, a clear peak was observed at 97 K. At the end of the transition (87 K), the $ErFeO_3$ changes from the metastable state to the stable state for the lower temperature (Γ_2), causing another steep decrease in the moment. When the static magnetic field increases to 100 Oe, the steps in the two-step process become more separated.

With further increase of the static magnetic field to 500 Oe and 1000 Oe, two completely discontinuous steps were observed at the beginning and end of the transition. When the static magnetic field is applied, especially for a higher field, it may couple with vector $\boldsymbol{F}$ and pull the sublattice magnetization towards the field direction, eventually inducing a spin-flip transition.[26] During the spin reorientation, for $ErFeO_3$, with smaller anisotropy of the metastable state, the FM vector $\boldsymbol{F}$ is possibly driven towards the field direction by the larger static magnetic field, resulting in deviation from the *ac*-plane. The initial and the final magnetic states, Γ_4 and Γ_2, remain unchanged, however, with larger anisotropy and a stronger pinning force. Therefore, the FM vector $\boldsymbol{F}$ rotates discontinuously, inducing two completely discontinuous steps at the beginning and end of this transition. This result suggests that the spin reorientation process could be manipulated by an external magnetic field and that a magnetic switching device could be designed based on effective control of the spin reorientation process.

The complex dynamic susceptibility of $ErFeO_3$ single crystal has been investigated in order to discover the possible mechanism of its spin reorientation. The static magnetic field shows especially strong effects on the dynamic susceptibility of $ErFeO_3$ during the spin reorientation process. When zero magnetic field is applied, a plateau-like peak is observed in the spin reorientation region. A high static magnetic field drives the transition into two completely discontinuous steps, showing discontinuous rotation of the FM vector at the beginning and end of the transition. Changes in the magnetic anisotropy or the interaction between the external magnetic field and the FM vector in $ErFeO_3$ during the transition account for this intriguing behaviour. Novel magnetic switching devices could be designed based on this work.

Hui Shen would like to acknowledge the financial support provided by the National Natural Science Foundation of China (Nos. 51002097, 51002087, and 51372257), the National Key Basic Research Program (No. 2011CB612310), the Shanghai Commission of Sciences and Technology (No. 11JC1412400), and the Shanghai Education Commission (Nos. 11YZ223 and J51504). Z. X. Cheng thanks the Australian Research Council for support through a Future Fellowship. S. X. Cao and S. J. Yuan thank the National Science Foundation of China for support (Nos. 50932003 and 51372149). The authors would like to thank Dr. Tania Silver for carefully polishing the English of this paper.

[1]Y. Tokunaga, N. Furukawa, H. Sakai, Y. Taguchi, T. Arima, and Y. Tokura, Nat. Mater. **8**, 558 (2009).
[2]A. V. Kimel, B. A. Ivanov, and R. V. Pisarev, Nat. Phys. **5**, 727 (2009).
[3]A. V. Kimel, A. Kirilyuk, P. A. Usachev, R. V. Pisarev, A. M. Balbashov, and Th. Rasing, Nature **435**, 655 (2005).
[4]R. Z. Zhou, Z. M. Jin, G. F. Li, G. H. Ma, Z. X. Cheng, and X. L. Wang, Appl. Phys. Lett. **100**, 061102 (2012).
[5]Z. M. Jin, Z. Mics, G. H. Ma, Z. X. Cheng, M. Bonn, and D. Turchinovich, Phys. Rev. B **87**, 094422 (2013).
[6]Y. Tokunaga, S. Iguchi, T. Arima, and Y. Tokura, Phys. Rev. Lett. **101**, 097205 (2008).
[7]A. Stroppa, M. Marsman, G. Kresse, and S. Picozzi, New J. Phys. **12**, 093026 (2010).
[8]J.-H. Lee, Y. K. Jeong, J. H. Park, M.-A. Oak, H. M. Jang, J. Y. Son, and J. F. Scott, Phys. Rev. Lett. **107**, 117201 (2011).
[9]P. Mandal, V. S. Bhadram, Y. Sundarayya, C. Narayana, A. Sundaresan, and C. N. R. Rao, Phys. Rev. Lett. **107**, 137202 (2011).
[10]R. V. Pisarev, A. S. Moskvin, A. M. Kalashnikova, and Th. Rasing, Phys. Rev. B **79**, 235128 (2009).
[11]B. Berini, A. Fouchet, E. Popova, J. Scola, Y. Dumont, N. Franco, R. M. C. da Silva, and N. Keller, J. Appl. Phys. **111**, 053923 (2012).
[12]L. T. Tsymbal, Ya. B. Bazaliy, V. N. Derkachenko, V. I. Kamenev, G. N. Kakazei, F. J. Palomares, and P. E. Wigen, J. Appl. Phys. **101**, 123919 (2007).
[13]B. Rajeswaran, D. I. Khomskii, A. K. Zvezdin, C. N. R. Rao, and A. Sundaresan, Phys. Rev. B **86**, 214409 (2012).
[14]S. J. Yuan, Y. B. Wang, M. J. Shao, F. F. Chang, B. J. Kang, Y. Isikawa, and S. X. Cao, J. Appl. Phys. **109**, 07E141 (2011).
[15]F. Hong, Z. X. Cheng, J. L. Wang, X. L. Wang, and S. X. Dou, Appl. Phys. Lett. **101**, 102411 (2012).
[16]L. T. Tsymbal, V. I. Kamenev, Ya. B. Bazaliy, D. A. Khara, and P. E. Wigen, Phys. Rev. B **72**, 052413 (2005).
[17]L. T. Tsymbal, Ya. B. Bazali, G. N. Kakaze, Yu. I. Nepochiatykh, and P. E. Wigen, Low Temp. Phys. **31**, 277 (2005).
[18]A. V. Kimel, A. Kirilyuk, A. Tsvetkov, R. V. Pisarev, and Th. Rasing, Nature **429**, 850 (2004).
[19]J. A. de Jong, A. V. Kimel, R. V. Pisarev, A. Kirilyuk, and Th. Rasing, Phys. Rev. B **84**, 104421 (2011).
[20]K. Yamaguchi, T. Kurihara, Y. Minami, M. Nakajima, and T. Surmoto, Phys. Rev. Lett. **110**, 137204 (2013).
[21]P. Mandal, C. R. Serrao, E. Suard, V. Caignaert, B. Raveau, A. Sundaresan, and C. N. R. Rao, J. Solid State Chem. **197**, 408 (2013).

[22]X. C. Kou, R. Grössinger, G. Hilscher, H. R. Kirchmayr, and F. R. de Boer, Phys. Rev. B **54**(9), 6421 (1996).
[23]R. W. Grant and S. Geller, Solid State Comm. **7**, 1291 (1969).
[24]Y. Sundarayya, P. Mandal, A. Sundaresan, and C. N. R. Rao, J. Phys.: Condens. Matter **23**, 436001 (2011).
[25]S.-J. Kim, G. Demazeau, I. Presniakov, and J.-H. Choy, J. Solid State Chem. **161**, 197 (2001).
[26]Ya. B. Bazaliy, L. T. Tsymbal, G. N. Kakazei, A. I. Izotov, and P. E. Wigen, Phys. Rev. B **69**, 104429 (2004).
[27]R. L. White, J. Appl. Phys. **40**(3), 1061 (1969).
[28]F. Grandjean, O. Isnard, and G. J. Long, Phys. Rev. B **65**, 064429 (2002).
[29]A. Bombik and A. W. Pacyna, J. Magn. Magn. Mater. **220**, 18 (2000).
[30]A. Bombik, B. Leśniewska, and A. W. Pacyna, J. Magn. Magn. Mater. **250**, 325 (2002).